Physics – Uspekhi **58** (4) 384 – 397 (2015)

METHODOLOGICAL NOTES PACS numbers: **91.30. – f**, 91.30.Px

Foreshocks and aftershocks of strong earthquakes in the light of catastrophe theory

A V Guglielmi

DOI: 10.3367/UFNe.0185.201504f.0415

Contents

Abstract. In this review, general ideas and specific results from catastrophe theory and the theory of critical phenomena are applied to the analysis of strong earthquakes. Aspects given particular attention are the sharp rise in the fluctuation level, the increased reactivity of dynamical systems in the near-threshold region, and other anomalous phenomena similar to critical opalescence. Given the lack of a sufficiently complete theory of earthquakes, this appears to be a valid approach to the analysis of observations. The study performed brought out some nontrivial properties of a strong-earthquake source that manifest themselves both before and after the main rupture discontinuity forms at the mainshock. In the course of the analysis of the foreshocks and aftershocks, such concepts as the round-the-world seismic echo, the cumulative effect of converging surface waves on the epicentral zone, and global seismicity modulation by Earth's free oscillations are introduced. Further research in this field is likely to be interesting and promising.

Keywords: earthquake, critical phenomena, bifurcation, surface waves, spheroidal oscillations, cumulative effect, modulation of seismicity

A V Guglielmi Shmidt Institute of Physics of the Earth, Russian Academy of Sciences, ul. B. Gruzinskaya 10, 123995 Moscow, Russian Federation
E-mail: guglielmi@mail.ru

Received 23 May 2014
Uspekhi Fizicheskikh Nauk **185** (4) 415 – 429 (2015)
DOI: 10.3367/UFNr.0185.201504f.0415
Translated by S D Danilov; edited by A Radzig

1. Introduction

Earth's solid shell (lithosphere) is sometimes shaken by sudden shocks — earthquakes [1]. A strong earthquake is called a mainshock or main stroke if it is followed by less powerful earthquakes called aftershocks. Rather often, but not always, the mainshock is preceded by a foreshock. This classical triad, namely foreshocks, the mainshock and aftershocks, will be considered here from the standpoint of the catastrophe theory, but we need to make a set of preliminary remarks first.

Sometimes, within a more or less compact group of tremors it is difficult to single out the main one. In seismology, such a group is referred to as an earthquake *swarm*. And although there are no doubts that swarms can also be productively analyzed from the general standpoint of the theory of critical phenomena and the theory of catastrophes, in this paper our attention will be concentrated on the classical triad alluded to above.

The strength of an earthquake is routinely characterized by its magnitude M [2]. The magnitude M is related to the energy E of seismic waves released on geologic fault fracture in rock in the epicentral zone of the earthquake, as follows:

$$\lg E = \alpha + \beta M\,. \tag{1}$$

Here, $\alpha = 11.8$, $\beta = 1.5$, and the energy E is expressed in ergs [3]. By definition, the magnitude of the mainshock exceeds those of foreshocks and aftershocks. With this only exception, the relationships between the magnitudes of earthquakes in the classical triad vary in wide limits from case to case. According to observations, foreshocks are commonly weaker than aftershocks. It has also been detected that

maximum magnitude of aftershocks is, on average, weaker than the magnitude of the mainshock by the quantity $\Delta M \sim 1$ [4]. This implies that the energy of the most powerful aftershock is smaller than the energy of the mainshock by a factor of approximately 30.

The distribution of earthquakes over magnitudes is subject to the Gutenberg–Richter law [5]

$$\lg N = a - bM\,. \tag{2}$$

Here, N is the mean number of earthquakes with magnitude greater than or equal to M in one seismically active region or another for a certain time interval (commonly, a year). We present, for information, typical values of parameters of the distribution: $a = 5$, $b = 1$. Interestingly, for foreshocks, the value of b is smaller than the typical one by a factor of between one and a half and two. This gives a rationale to consider a substantial reduction in b in a region with the passage of time as one of prognostic indications of a strong earthquake that will happen there soon [6, 7].

A question arises as to whether it is possible, knowing the magnitude M, to conclude with certainty that the earthquake is strong in the sense formulated above, i.e., that it will be accompanied by aftershocks. Generally speaking, the answer is no. For example, an earthquake with magnitude $M = 7.2$, which is strong in a broad sense, was only the aftershock of an earthquake with magnitude $M = 9$ that took place near the Sumatra coast on 26 December 2004 [8]. Even a stronger aftershock ($M = 7.9$) was observed after an earthquake with magnitude $M = 9$ near the eastern coast of Honshu on 11 March 2011 [9]. In what follows, we will return to the analysis of these aftershocks, because they turned out to be interesting from the standpoint of catastrophe theory. It should be mentioned here that in this paper we will not touch, for reasons easily understood, the question about numerous victims and devastating economic consequences of the earthquakes mentioned.

There is extensive literature on various aspects of earthquake physics. A list, by far incomplete, may be acquainted in monographs [1–3, 6,7]. Several papers on earthquakes have been published on the pages of *Physics–Uspekhi* [10–16]. We briefly mention Ref. [16], since its name partly coincides with that of this article. We would like to avoid any misunderstanding which may be caused by the ambiguity of the term 'catastrophe'. In Ref. [16], in order to mitigate earthquakes, it is proposed that microwave radiation be acted on rocks, while earthquakes are treated as ecological catastrophes leading to casualties. In contrast, we consider earthquakes on their own from the standpoint of the critical phenomena and catastrophe theories. We note in passing that we will leave aside not only the difficult question of anthropogenic action on the lithosphere aiming to prevent earthquakes, but also the currently topical question related to the search for mechanical and electromagnetic forerunners for earthquake prognosis (see, for example, Refs [17–27]). Both these questions are important from the practical side, but in this paper we pursue a much more modest goal.

It should be kept in mind that catastrophe theory, the foundations of which were laid in the 1960s, studies the singularities of smooth maps and bifurcations in dynamical systems [28–30]. The state of a system is described phenomenologically by a set of functions $\psi_j(t, c_\alpha)$, $j = 1, 2, \ldots, n$ which depend on time and the so-called governing parameters c_α, $\alpha = 1, 2, \ldots, m$. A catastrophe occurs as a sharp change in ψ_j following a smooth change in c_α. The system is characterized by the potential function $U(\psi_j, c_\alpha)$ which depends on the state and governing parameters. The equation

$$\frac{\mathrm{d}\psi_j}{\mathrm{d}t} = -\frac{\partial U}{\partial \psi_j} \tag{3}$$

describes the system's evolution. An important task is the analysis of critical points of the potential function. On approaching a critical point, the Hessian of the potential function tends to zero:

$$\det \frac{\partial^2 U}{\partial \psi_i \partial \psi_j} \to 0\,. \tag{4}$$

A real physical system (for example, a site of a future earthquake) in the coarse of its smooth evolution may approach a threshold followed by a catastrophe (in our case, the formation of a fault fracture in rock). The observation suggests that catastrophes often happen unexpectedly. In practice, one cannot foresee an actual catastrophe in many cases. In such circumstances, it is important to know that a theory exists which unambiguously points to a set of attributes related to the approaching change in the system's state. These attributes are called catastrophe flags, meaning that the system behaves as if it 'raises signal flags' telling of an approaching radical change [29]. A rather typical factor of this type is an anomalous growth in fluctuations as the system gets closer to the critical point. Notice that this property of non-equilibrium dynamical systems was known in physics long before the appearance of catastrophe theory. For example, critical opalescence [31] presents an apparent manifestation of anomalous growth in fluctuations at phase transitions in fluids. The concept of catastrophe flags has been successfully used to analyze foreshocks. The respective results are presented in Section 2.

While the idea of flags gave the possibility of viewing the dynamics of foreshocks from a different angle, the idea of triggers helped to uncover the features of aftershocks unknown previously. We call a *trigger* a relatively weak action that leads to a considerable, generally speaking, catastrophic change in the system's state. This definition is not truly rigorous, yet it is apparent. Here is an example clarifying the essence. For eight thousand years, high in the mountains of Trans-Ili Alatau, was Lake Issyk, called a 'jewel in a granite cast'. This lake has disappeared as a result of an ecological catastrophe. The author was in that area as a member of an expedition launched by the Institute of Earth Physics, AS USSR and turned out to be one of the last to have seen this lake, so rare in its beauty. On Sunday, 7 July 1963, a vigorous mudflow slid into the lake and literally thrust it, splashing out an immense mass of water, downhill. The mudflow was a trigger, and the catastrophe took place because Lake Issyk was in a metastable state.

The recollection of the catastrophe at Lake Issyk hinted at how to create a simple model which will help us to introduce the concept of endogenic and exogenic triggers. Assume, to begin with, that triggers are absent. As a seed, we use a 'fold' catastrophe in the classification of Thom [28], or of the A_2 type in the Arnol'd classification [30]. The potential function assumes the form $U(\psi) = U(0) - c_1\psi + c_2\psi^2 - c_3\psi^3$, with

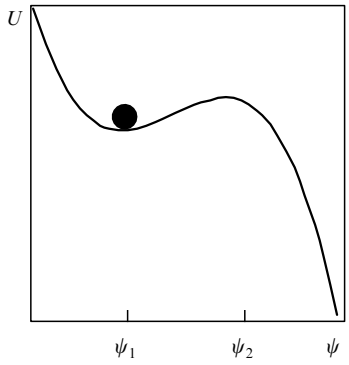

Figure 1. Potential relief in the form of a cubic parabola. The black ball resides in a metastable state. A critical transition may occur under the action of an endogenic or exogenic trigger.

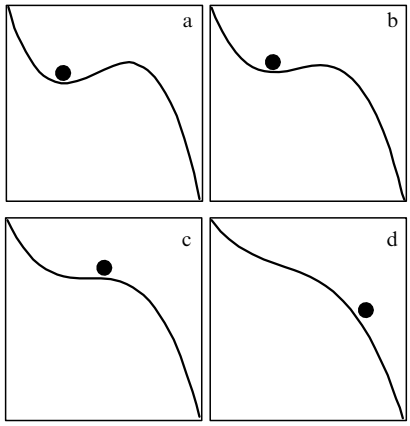

Figure 2. Change in the potential relief with time leading to a catastrophe. From a metastable state (a, b) through the bifurcation (c), the system arrives at a nonequilibrium state (d).

$\psi \geqslant 0, c_\alpha \geqslant 0, \alpha = 1, 2, 3$. In other words, the potential has the form of a cubic parabola (Fig. 1). The minimum and maximum of the potential correspond to the stable (ψ_1) and unstable (ψ_2) equilibrium states of the system ($\mathrm{d}\psi/\mathrm{d}t = 0$). The state ψ_1 is metastable. This implies that, under the action of noise, characteristic of any real system, or under the action of external force, the system may undergo a phase transition $\psi_1 \to \psi > \psi_2$ and in that manner lose its equilibrium ($\mathrm{d}\psi/\mathrm{d}t > 0$).

Thus, we have the simplest phenomenological model that imitates the metastable state of a dynamical system. Models of this type have been widely discussed previously in analyses of magnetospheric oscillations [32, 33]. It seems likely that such models, with known reservations, can be used while discussing fluctuational and critical phenomena in the lithosphere [34–37]. Such a model, even in a rather primitive form as above, offers, for example, a metaphor for thinking about the process leading up to an earthquake. This model can be used, albeit with caution, as an auxiliary scheme of a certain kind. We will dwell on this in some detail.

Obviously, the system may lose equilibrium under the action of noise or external forcing if the governing parameters c_α slowly vary with time such that the height of a potential barrier $\Delta U = U(\psi_2) - U(\psi_1)$ monotonically declines. Figure 2 illustrates this decrease. Figure 2c depicts the potential at the moment of critical transition from the metastable state (Fig. 2a and b) to the nonequilibrium state (Fig. 2d). However, if, ignoring the obviously gross character of the seed model, we tried to describe with its help the process leading to an earthquake, it would then turn out that the moment of an earthquake is associated with the moment of critical transition. This would be a mistake. Indeed, in Earth's crust, or more precisely, on the site of a future earthquake, a certain background level of seismic fluctuations is present. Under their influence, the earthquake may take place substantially earlier than the moment of critical transition, i.e., at the moment shown in Fig. 2b, in contrast to 2c. In other words, on approaching the bifurcation point defined by the condition $\Delta U = 0$, fluctuations in the stresses in rock may become a trigger causing earthquakes.

To describe the effect of fluctuations on the system, we replace dynamical equation (3) with the stochastic Langevin equation

$$\frac{\mathrm{d}\psi}{\mathrm{d}t} = -\frac{\partial U}{\partial \psi} + \xi(t)\,. \tag{5}$$

Here, the additive term $\xi(t)$ is a random function with a zero mean, and $\langle \xi(t')\xi(t'') \rangle = 2D\delta(t' - t'')$, where $\delta(t)$ is Dirac's delta-function, and the angular brackets stand for statistical averaging. The new phenomenological parameter D of the model is proportional to the intensity of seismic noises in the vicinity of 'ripening' earthquakes. (One may similarly take into account endogenic triggers in the form of multiplicative noise, yet we leave this aside, directing the interested reader to monograph [38].) A strong fluctuation $\xi(t)$ will excite the critical transition at a certain instant of time. We will refer to it as a spontaneous transition, and to the fluctuation $\xi(t)$ as an endogenic trigger. The probability of spontaneous transition is proportional to $\exp(-\Delta U/D)$, i.e., it is exponentially small if the potential barrier is sufficiently high [39].

Further generalization consists in accounting for the external forces $f(t)$ exerted on the system:

$$\frac{\mathrm{d}\psi}{\mathrm{d}t} = -\frac{\partial U}{\partial \psi} + \xi(t) + f(t)\,. \tag{6}$$

On approaching the bifurcation point, the barrier height ΔU decreases monotonically. As a consequence, the reactivity of the dynamical system increases sharply close to the threshold. In this state, even a weak external perturbation can trigger a catastrophe. Such a critical transition can be naturally referred to as induced, and the respective trigger, $f(t)$, as exogenic. If $f = 0$, the probability of catastrophe is exponentially small, as already mentioned above. If $f \neq 0$, the probability may increase considerably, even for a relatively weak amplitude of external force. In an important special case of periodic action, the transition probability increases by a factor of $\exp(F\Delta\psi/D)$, where $F = \langle 2f^2 \rangle^{1/2}$, and $\Delta\psi = \psi_2 - \psi_1$ is the width of the inflection zone of the potential relief [40].

The exogenic triggers of geocatastrophes can be natural or artificial, pulse or periodic, and of terrestrial or cosmic origin. The related literature is vast (see, e.g., monographs [41, 42] and the references cited therein). We will consider below two non-trivial triggers: the round-the-world seismic echo (Sections 3 and 4), and Earth's spheroidal oscillations (Section 5). The first of these triggers is a pulse one, and the second is periodic. They are both excited by the mainshock of earthquakes and influence the activity of aftershocks.

2. Foreshocks

2.1 Growth in foreshock activity three hours prior to the mainshock

Foreshocks as mechanical forerunners of a strong earthquake are formed at the final stage of the seismic cycle [19]. Various electromagnetic forerunners are also observed during the final stage (see the classical works [17, 18] and the recent publications [24–27]). Here, we consider the foreshock dynamics within the last several hours of the final stage [37].

A compeling motive for studying foreshocks during the last hours before the mainshock was provided by the results of the analysis of ultralow-frequency electromagnetic oscillations recorded by the measuring facility at the North Caucasus Geophysical Observatory [24, 25]. In the course of the analysis, an increase in activity of oscillations has been noticed 2–4 hours prior to strong earthquakes. The attempt in Ref. [37] to reveal specific properties in the foreshock dynamics related directly or indirectly to the elevated activity of electromagnetic oscillations is thus rather natural. The result of this quest turned out to be fairly interesting.

The analysis of foreshocks that took place from 1964 to 2009 was based on the data of the earthquake catalogue of the International Seismological Centre (ISC) (http://www.isc.ac.uk). Strong earthquakes with magnitudes $M \geqslant 7.5$ have been singled out from the catalogue. Their occurrence times were used as a reference to synchronize foreshocks. The foreshocks were identified in the catalogue by a combination of three factors, namely, the place, time, and magnitude. An earthquake was attributed to foreshocks if its epicenter was separated from the reference epicenter by less than 600 km. Only those earthquakes that occurred less than 10 h prior to the reference were counted. Finally, a natural bound on their magnitude was imposed: $M < 7.5$.

The result of the selection and accumulation of foreshocks is presented in Fig. 3. Its vertical axis plots the magnitude, and the horizontal axis plots time, with zero associated with the instant of time the reference earthquake took place. The series plotted in Fig. 3 was subject to an additional strong constraint from below on the amplitude of foreshocks: $5 \leqslant M < 7.5$. As a consequence, Fig. 3 plots the time distribution of strong foreshocks in the epicentral zones of strong earthquakes.

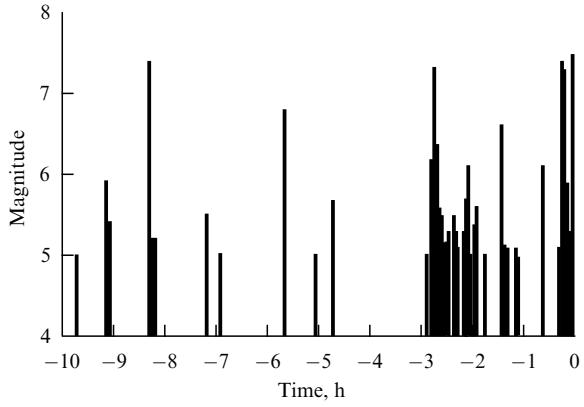

Figure 3. Strong foreshocks ($5 \leqslant M < 7.5$) at the final stages prior to strong earthquakes ($M \geqslant 7.5$) based on the ISC catalogue data (1964–2009). The zero mark corresponds to the instant of the mainshock. The result was obtained by epoch superposition analysis.

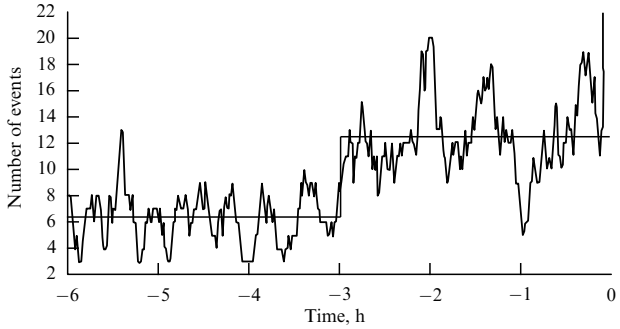

Figure 4. Averaged dynamics of foreshocks ($M < 7.5$) in epicentral zones of strong earthquakes ($M \geqslant 7.5$). Zero time corresponds to the mainshock instance. The horizontal lines depict mean values of the number of foreshocks.

We see that the distribution of foreshocks with time is inhomogeneous. Only rare events take place earlier than −3 h, but a sharp increase in the activity of foreshocks is observed after −3 h. This is reminiscent of the increase in activity of electromagnetic oscillations approximately 3 h before the mainshock [24, 27]. We do not claim the presence of a causal relationship here, as there are no sufficient grounds for that. The point is only that, in all probability, certain parallels exist in the course of electromagnetic and mechanical processes during the final stage of events culminating in an earthquake.

The sharp increase in seismic activity is also identified for a less constrained selection of foreshocks. If we lift the constraint on the foreshock magnitude from below, we get the result plotted in Fig. 4. We see the averaged dynamics of foreshocks ($M < 7.5$) in epicentral zones of strong earthquakes ($M \geqslant 7.5$). The plot is constructed as follows: the number of foreshocks within an 11 min window was counted, with the window running along the horizontal axis with a 1-min step. The measured means and standard deviations prior to (and after) the time instant of −3 h are equal to 6.3 (12.5) and 1.95 (3.01), respectively. From these estimates, taking into account the sample volumes, the error bars for possible deviations of measured values from the true mean are evaluated to be 6.3 ± 0.436 prior to −3 h, and 12.5 ± 0.68 after the instant of −3 h. The twofold increase in foreshock activity three hours before the mainshock is beyond any doubt.

The fact itself of the appearance of foreshocks and growth in their activity can be more or less comprehended in the light of catastrophe theory. However, the jump in the activity of foreshocks 3 h prior to the mainshocks looks somewhat puzzling. We will try to attach some physical sense to this observation in Section 2.3.

2.2 Critical retardation

We pay attention to the fact that, as time progresses, the quasiperiod of fluctuations in Fig. 4 substantially increases. We would like to relate this feature to a prediction from catastrophe theory: so-called mode softening. Its essence hinges on the fact that, on approaching the bifurcation, the Hessian (4) of the potential function tends to zero. Hence, it follows that at least one of the eigenfrequencies of the dynamical system is lowered [29]. This rather general property came to be known as 'mode softening' or 'critical slow-down of a process before catastrophe'.

As is seen from Fig. 5, there are indeed indications that the characteristic frequency of fluctuations in foreshock

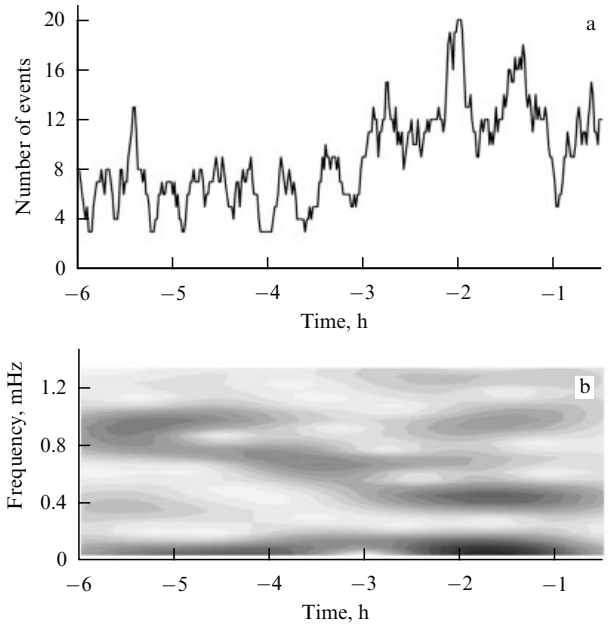

Figure 5. Variation of the number of foreshocks (a) and the respective dynamical spectrum (b).

activity gets lower at the final stage before the mainshock. Figure 5a presents the variability of foreshocks, and Fig. 5b displays the respective dynamical spectrum. It cannot be ruled out that the dynamical spectrum points to a certain mode softening in the zone of earthquake preparation before the onset of the rock mainline rupture, in accordance with the catastrophe theory.

We conclude this section with a compeling comparison. Namely, we juxtapose Fig. 5, supposedly confirming a catastrophe theory prediction, with Fig. 13 of Ref. [43] (that does not resort to the catastrophe theory). According to the latter figure, the characteristic frequency of oscillations in seismic activity drops by an octave in the interval of several years preceding a strong earthquake. In that case, the frequency of oscillations is on the order of several dozen nanohertz. Here, we are dealing with fluctuations in the millihertz range (see Fig. 5). A detailed comparison of dynamical spectra reveals that there is a difference in frequencies by four orders of magnitude between our case and the one considered in Ref. [43]. The fact that in both cases the frequency drops by one octave would be of no relevance were it not for one interesting circumstance: namely, the time intervals where the change is observed also differ by four orders of magnitude, similarly to the difference in the characteristic frequencies of oscillations. Could it be that we are dealing with a scaling here? We cannot answer this question yet, but it fully deserves further study.

2.3 Round-the-world seismic echo

Making all necessary stipulations, we embark on presenting a hypothesis about the origin of the sharp jump in the foreshock activity approximately 3 h in advance of the mainshock. The hypothesis came to be during attempts to attach some physical sense to the three-hour time interval. A comparative analysis of the variants of interpretation allows formulation of a proposition that the delay is of kinematic origin, with the interval being the time it takes the Rayleigh surface wave to travel across the surface of Earth.

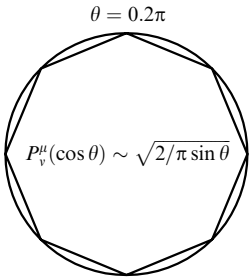

Figure 6. Schematic of rays of a round-the-world echo created by surface and bulk waves (smooth and broken lines, respectively). In the center, the angular dependence of associated Legendre polynomials is given; the amplitude of seismic oscillations is proportional to them.

Indeed, let us take into account that foreshocks excite surface elastic waves. Let us further note that waves propagating from the foreshock epicenter with a characteristic speed of 3.7 km s^{-1} return to the epicenter of the future mainshock in approximately three hours, having accomplished a full circle around Earth. We will call this phenomenon the round-the-world seismic echo (Fig. 6). (Something similar is observed as a round-the-world radio echo in the propagation of short radio waves [44].) Now, let us take into account that the amplitude of the echo continuously increases on approaching the epicenter. Indeed, the Legendre polynomial $P_\nu^\mu(\cos\theta)$ is proportional to the amplitude of oscillations at the angular distance θ from the foreshock epicenter [45]. Asymptotically [46], $P_\nu^\mu(\cos\theta) \sim \sqrt{2/\pi \sin\theta}$, i.e., the amplitude of the round-the-world echo increases as the center is approached: $\theta = 2\pi$ (Fig. 6). It should be clear that the amplitude never reaches infinity, in contrast to the predictions of the asymptotic theory elaborated for the model of spherically symmetric Earth. Owing to diffraction and spherical and chromatic aberration, the wave amplitudes stay bounded. Nevertheless, it is plausible to assume that approximately three hours after the foreshock the effect of converging seismic waves stimulates the formation of a fault rupture in rock, followed by a powerful earthquake.

It should be remembered that the above-proposed hypothetical sequence of events unfolds against the background of a dynamical system rapidly evolving into a total catastrophe. Catastrophe theory definitely predicts an anomalous growth in stress fluctuations in rock at this stage of evolution. In the absence of external actions, some sufficiently powerful fluctuation at a particular instant of time in one way or another will result in a mainline rupture, i.e., serve as an endogenic trigger. A question is then formulated as to whether or not the mainline rupture can happen before this instant under the action of the round-the-world echo excited by the foreshock. An indirect argument in favor of the hypothesis that such events sometimes do happen in the three-hour lag of the mainshock relative to the point in time at which the sharp increase in the foreshock activity emerges. Yet another indirect argument in its favor is that the round-the-world echo from the mainshock induces aftershocks, but this will be addressed in Section 4.

Let us make the empirical basis of our hypothesis more illustrative. With this intention, we select a relevant fragment in Fig. 3, transform the magnitude M to energy E using formula (1), and carry out smoothing by summing the energy within 9-minute intervals which are sequentially shifted in 1-min time steps. The result is displayed in Fig. 7a (the

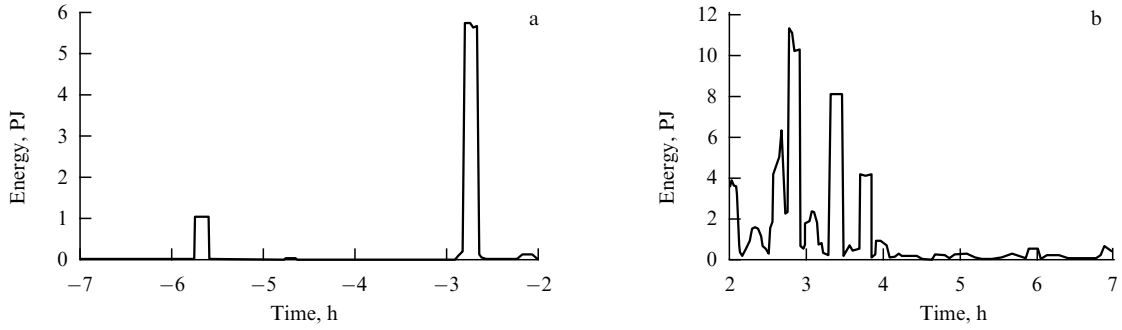

Figure 7. Energies of foreshocks (a) and aftershocks (b) in epicentral zones of strong earthquakes ($M \geqslant 7.5$).

comparison of Figs 7a and 7b is postponed until Section 4). We see a strong peak in energy release at the instant of time falling on -2.8 h. The interval of 2.8 h corresponds to the time it would take a seismic wave to make a complete circle around Earth at a speed of 4 km s^{-1}, which is in sound agreement with the characteristic speed of surface waves known from computations and observations.

We point to yet another observational fact in favor of the hypothesis being considered. Namely, as an addendum to the analysis of global seismicity displayed in Fig. 7, we present in Fig. 8 the result of regional seismicity analysis based on the data on earthquakes in California listed in the catalogue http://www.data.scec.org/ (1983–2008) and http://www.ncedc.org/ (1968–2007). The time instants of mainshocks with magnitudes $M \geqslant 6$ are taken as references synchronizing foreshocks and aftershocks (zero time in the figure). The energy of earthquakes was averaged over 20-minute intervals, which were shifted in one-minute time steps. The energy of the mainshocks was discarded and is not shown in Fig. 7. (In some events, the energy of the mainshocks reached several petajoules.) Approximately three hours before the zero mark, a peak in foreshock energy release is observed, which, arguably, triggered a part of the mainshocks.

To conclude this section, we clarify that the round-the-world echo is formed, generally speaking, not only by surface waves, but also by bulk waves multiply reflected from Earth's surface and forming a wave structure resembling that of a whispering gallery (for whispering gallery modes, see, for example, monograph [47]). From the standpoint of ray theory, the amplification of bulk waves in the epicenter will take place on their return to the initial point, being resonantly shorted to themselves (see Fig. 6). This question deserves a detailed analysis; however, we need to stress that computations of the monodromy matrix and multipliers will be unwieldy if the analysis involves a more or less realistic model of Earth's internal structure. At present, one can firmly argue only that an echo in bulk waves, were it indeed started, should return to the epicenter earlier than an echo in surface waves. A theoretically plausible exclusion could be an echo in very short waves, which tightly lean to Earth's surface, forming a structure like a thin wave film. However, because of strong absorption on multiple reflections from Earth's surface, the intensity of such an echo will, most probably, be negligibly small.

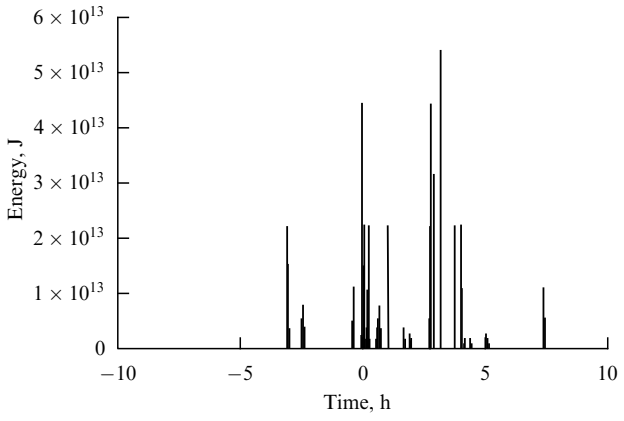

Figure 8. Energies of foreshocks and aftershocks for strong earthquakes in California. The zero time corresponds to the moment of the mainshock.

3. Cumulative effect of converging surface waves

3.1 Converging waves

It is appropriate to make preliminary remarks concerning converging waves, albeit of a rather obvious character. It is known that the Sommerfeld radiation condition singles out retarded solutions of the wave equation, representing diverging waves at some sufficiently long distance from the sources. The Sommerfeld condition corresponds to the causality principle. Moreover, according to Zeldovich's idea, it proposes one possible explanation of time irreversibility (see, for example, book [48]). On the other hand, advanced solutions may make some sense, too. For example, Feynman, following Frenkel, used a half sum of retarded and advanced solutions to eliminate infinities in classical electrodynamics [49].

In this section, as follows from its title, we will be dealing with converging, instead of diverging, waves. To avoid possible misunderstandings, it is useful to turn to two simple examples showing that in the world around us the converging waves undoubtedly exist, and this in no way violates the Sommerfeld condition or causality principle.

Converging waves can be created artificially. An elementary example is the formation of waves inside a horizontal circle thrown strictly vertically on the water surface. The second example is directly relevant to our topic. Let us assume that a spherically symmetric elastic ball is excited by a point impact. To be more illustrative, imagine a meteorite colliding with the Moon. The surface waves diverge from the place of impact, reach the equator, and then travel as converging waves which focus on a point which resides diametrically

opposite to the impact point. The subsequent evolution is rather obvious. The waves diverge at the beginning but then converge on the point of impact.

A similarly formulated problem was considered in seismology in the framework of linear theory of elasticity (see, for example, Ref. [50]). Distinct from that, we are willing to discuss nonlinearity which is inevitably present in the vicinity of focal points for a sufficiently strong impact. The idea is that the cumulative action of surface waves converging on foci can entail a medium rupture. Since the two foci represent a pair of mutually antipodal points, we will symbolically call this the antipodal effect.

We will discuss the antipodal effect on Earth, the Moon, and Mercury, paying attention to the fact that for the physics of earthquakes of special interest is the case when the geological medium in the vicinity of the focus resides at the state of stress close to its fracture stress. In this case, seismic waves converging on a focus may act on the medium as a trigger which can induce a critical transition and cause an earthquake.

3.2 Antipodal effect on Earth

Antipodes were known back in ancient times; however, the antipodal effect as a wave phenomenon came on the scene only in 1957, after the USSR launched the first artificial Earth satellite. Millions of radio hobbyists received signals from the satellite, but special interest and excitement was caused by a considerable increase in the amplitude of radio waves as the satellite passed through the vicinity of the antipodal point [51]. It is clear enough that the propagation of surface seismic waves generated by an earthquake leads to an analogous effect. Indeed, it follows from geometrical considerations that in the linear approximation the wave amplitude is formed by the superposition of associated Legendre polynomials, the amplitude of which at asymptotics is proportional to $\sin^{-1/2}\theta$, i.e., has poles at the epicenter ($\theta = 2\pi$) and anti-epicenter ($\theta = \pi$). Here, as above, θ is the angular distance from the epicenter. The wave passes half of the round-the-world distance in 90 min for a characteristic propagation speed of 3.7 km s^{-1}. Accordingly, the increase in the amplitude of oscillations at the antipodal point and in its vicinity is expected approximately an hour and a half after the beginning of the earthquake.

We pointed out the formal analogy between antipodal effects for radio and seismic waves. But this analogy is incomplete. There are two distinctions which are essential in our context. First, the effect of radio wave amplification was only observable when the satellite passed in the vicinity of the point that is diametrically opposite to that of the reception, i.e., at $\theta = \pi$. At $\theta = 2\pi$, the round-the-world signal was masked by the direct signal from the satellite transmitter. Second, the antipodal radio signal was linear, while we anticipate nonlinear manifestations induced by converging seismic waves.

The ideas presented above were first employed in Ref. [34] in an attempt to discover the nonlinear antipodal effect of seismic waves at antiepicenters of strong earthquakes. For the search, the coordinates of epicenters, occurrence times and magnitudes of earthquakes listed in the ISC catalogue were taken and the so-called superposed epoch analysis was applied (see, for example, Ref. [52]). The antipodal zone was selected as a spherical segment with the radius $\pi - \theta_0$ and its center at the point $\theta = \pi$. Further, the ISC catalogue was surveyed to count the number of earthquakes with magnitudes $M < M_*$ occurring in this segment following a strong earthquake with a magnitude $M \geqslant M_*$ and the epicenter at $\theta = 0$. The quantities θ_0 and M_* were chosen experimentally, so as to visualize the antipodal effect, were it possible at all with this approach. After some trials and errors, the optimal values of $M_* = 6$ and $\theta_0 = 160^\circ$ were found, which corresponds to an antipodal zone of 20° radius. The beginning of an epoch with a duration of 11 h was taken as the occurrence time of an earthquake with magnitude $M \geqslant M_*$. About 7000 epochs were selected within the time period from 1964 to 2006. For each epoch, the number of earthquakes with magnitudes $M < M_*$ was counted, occurring each one-minute interval in the respective antipodal zone.

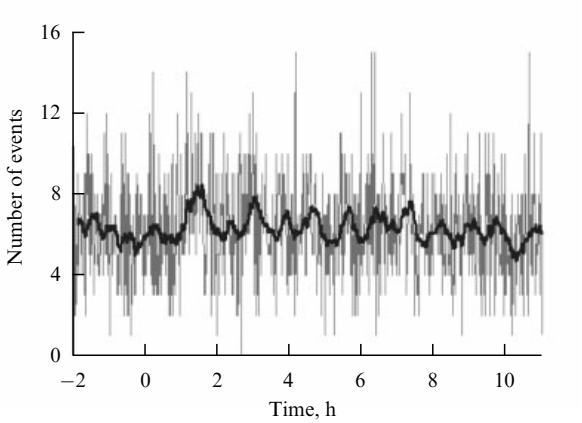

Figure 9. Averaged dynamics of weak earthquakes ($M \leqslant 1$) in the antipodal zone during the first two hours before and 11 hours after strong earthquakes ($M \geqslant 6$). The thick line is the result of a running mean over 20 points.

The result of epoch superposition is given in Fig. 9. The thick solid line was obtained as a running mean over 20 points. A noticeable maximum in the number of earthquakes in the antipodal zone was detected within approximately 90 min of the reference time. At first glance, this corresponds to expectations, but the effect is small in the following sense: in the overwhelming number of cases, only earthquakes with magnitudes $M \leqslant 1$, i.e., rather weak ones, were recorded in antipodal zones.

Trying to uncover why the antipodal effect is so weak in the vicinity of the $\theta = \pi$ point, the authors of Ref. [34] compared world maps of epicenters and anti-epicenters. It turned out that the antipodal points of earthquake epicenters are, as a rule, located in aseismic regions. This fact, interesting on its own, offered an explanation of the weakness of the effect at $\theta = \pi$. Moreover, it hinted that it is worthwhile to search for strong aftershocks in the vicinity of point $\theta = 2\pi$ approximately three hours after the mainshock, since it is known that a high stress level is preserved in Earth's crust long after the fault rupture. In some places, this level is close to the rock rupture strength, as witnessed by numerous aftershocks. It was therefore anticipated that the round-the-world echo of the mainshock may trigger strong aftershocks. The result of respective research matched the expectation; details will be postponed till Section 4.

3.3 Comparison with antipodal effects on the Moon and Mercury

The substantial effect of converging seismic waves on rock at an antiepicenter, i.e., at $\theta = \pi$, has been well known for a long time in planetology [53–55]. With the help of cosmic

instruments, vast destruction areas (landslides, hilly landscape) were discovered in places diametrically opposite to impact craters on the Moon and Mercury. On the Moon, for example, surface destructions have been discovered for the antipode of the Sea of Rains. On Mercury, whose surface resembles the lunar one, anomalous relief is observed in the area diametrically opposite to the Caloris Basin. It seems quite apparent that destructions are caused by the cumulative action of converging seismic waves excited by a meteorite impact.

Thus, antipodal effects on Earth, on the one hand, and on the Moon and Mercury, on the other hand, are similar to each other in that they originate from the momentum and energy concentration upon focusing converging seismic waves. As concerns their distinctions, they are rather obvious. On the Moon and Mercury, the effect of interest is caused by meteorite impacts in the distant past and is manifested as surface destructions in places diametrically opposing the impact sites, whereas on Earth the effect is observed in the present epoch as repeated shocks after strong earthquakes.

But why did the cumulative effect prove to be relatively weak in the vicinities of antiepicenters of strong earthquakes? We have explained it above by arguing that on Earth the antipodal zones of epicenters are located, as a rule, in aseismic areas. This is, however, insufficient, because on the Moon and Mercury considerable surface destructions are seen in the vicinities of antiepicenters, and these destructions, by all indications, are caused by the direct, rather than triggering, forcing of converging seismic waves. One may propose that the impact excitation of seismic waves by a meteorite is more efficient than in the case of earthquakes. One more argument is a weaker attenuation of seismic waves on the Moon and Mercury than on Earth.

4. Aftershocks

The mere fact of the emergence of numerous aftershocks indicates that after the mainshock the level of stresses in the Earth's crust remains high in the vicinity of epicenter over a long time period. The fault rupture causing the mainshock does not release the stresses accumulated earlier, but redistributes them over other areas of the earthquake vicinity, in this way increasing the probability for subsequent shocks to occur. Thus, it is the sequence of aftershocks for which there is a chance to find the trigger effects. In Sections 4.1 and 4.2 we will consider a pulse trigger, and in Section 5, a periodic one.

4.1 Analysis of the strongest earthquakes

We try to find the cumulative effect of converging surface waves in the sequence of aftershocks of the Sumatra–Andaman megaearthquake — one of the strongest at the beginning of the 21st century [36].

An earthquake with magnitude $M = 9.0$ took place in Southeast Asia on 26 December 2004 at 0:58:53 GMT. Figure 10 shows the position of the epicenter of this earthquake, located in the Indian Ocean, north of the island Simeulue close to the north-west coast of Sumatra. The strongest aftershock (magnitude $M = 7.2$) happened with a lag of 3 h 20 min with respect to the mainshock. The epicenter of the aftershock is also depicted in Fig. 10. The aftershock delay time is approximately the time it would take a surface wave to make a complete circle around Earth, which suggests that the round-the-world seismic echo signal, excited by the mainshock, could be the trigger causing the strong aftershock.

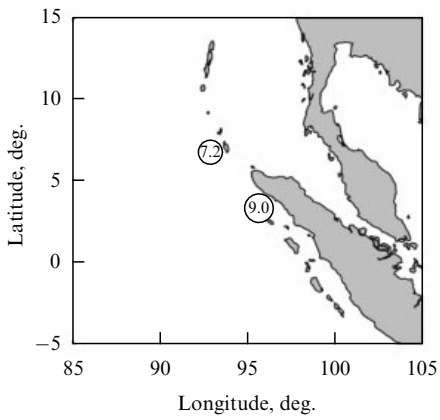

Figure 10. Map of the Northeast Indian Ocean with the epicenters of the mainshock of the Sumatra–Andaman earthquake ($M = 9.0$) and most powerful aftershock ($M = 7.2$).

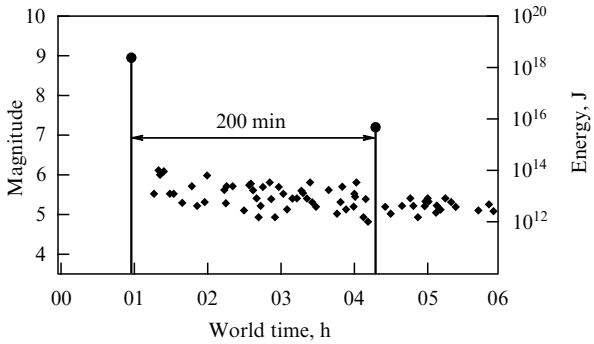

Figure 11. Sumatra–Andaman earthquake on 26.12.2004 and aftershocks in the interval of 5 h after the mainshock. The black circles mark the mainshock and the strongest aftershock.

Figure 11 demonstrates the aftershocks in the epicentral zone of 10° radius. The left ordinate shows the magnitude, and the right one marks the seismic energy computed by formula (1). Here, we took advantage of the earthquake data from the United State Geological Survey/National Earthquake Information Center — USGS/NEIC (http://neic.usgs.gov/neis/epic/epic_global.html). Within the interval of 5 h, 70 aftershocks were recorded. We see that the strongest aftershock ($M = 7.2$) took place 200 min after the mainshock. It cannot be excluded that it was induced by the round-the-world seismic echo. The idea is then that surface elastic waves generated by the Sumatra–Andaman earthquake caused this aftershock after completing a turn around Earth. We observe an approximate 20-min difference between the expected and recorded delay times. If our interpretation of the aftershock with magnitude $M = 7.2$ as an aftershock triggered by the round-the-world echo signal from the mainshock is valid, then the difference of 20 min between the expected and recorded times can naturally be explained by the overshoot phenomenon characteristic of the reaction of nonlinear dynamical systems on external actions [29].

Continuing our analysis, we draw attention to the possibility of the multiple propagation of surface waves around the globe and, respectively, the possibility of a repeated round-the-world echo of the mainshock. The repeated echo may induce an aftershock provided that some region of Earth's crust in the epicenter vicinity is in a subcritical state at the instant of the echo's arrival. Backed

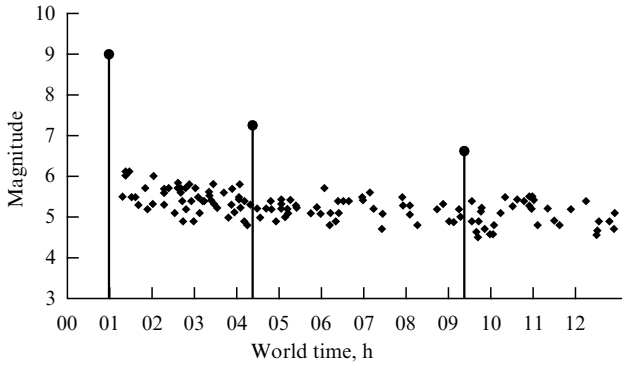

Figure 12. Sumatra–Andaman earthquake on 26.12.2004 and aftershocks within 12 hours after the mainshock. The black dots indicate the mainshock and two most powerful aftershocks.

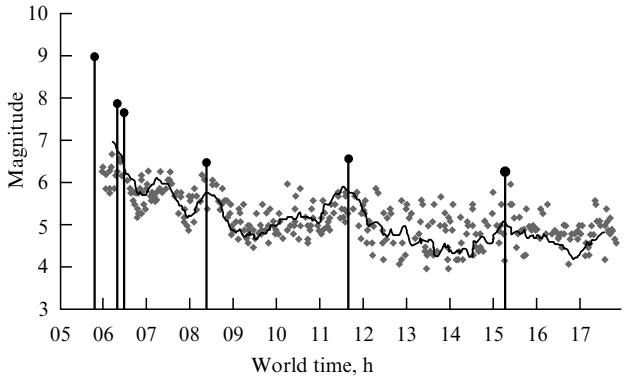

Figure 13. Earthquake in the Tohoku area on 11.03.2011 and aftershocks within 12 h after the mainshock. The black dots indicate the mainshock and the five strongest aftershocks. The continuous curve approximates the cloud of weaker aftershocks.

with these considerations, it was expected that the induced aftershock would appear within 6–7 h after the mainshock, but the expectation did not come true (Fig. 12). A second strong aftershock with magnitude $M = 6.6$ was recorded at 9 h 20 min, i.e., considerably later, namely 8 h 20 min past the mainshock, and 5 h after the first strong aftershock. Without appealing once again to the overshoot phenomenon, it should be suggested that the second strong aftershock happened as a result of the spontaneous transition under the action of an endogenic trigger.

It is of interest to juxtapose the aftershocks of the Sumatra–Andaman earthquake with the aftershocks of a similarly powerful earthquake in the region of Tohoku ($M = 9.0$), which took place on 11 March 2011 near the eastern coast of Honshu at 5 h 46 min GMT. The black circles in Fig. 13 mark the mainshock and five strong aftershocks. As concerns two powerful aftershocks at 6 h 16 min ($M = 7.9$) and 6 h 26 min ($M = 7.7$), they most probably occurred under the action of endogenic triggers. We, however, draw attention to the third, fourth, and fifth aftershocks recorded at 8 h 19 min, 11 h 36 min, and 15 h 13 min, with magnitudes $M = 6.5$, $M = 6.6$, and $M = 6.3$, respectively. The surprising regularity in their appearance suggests, for one thing, that we are dealing with earthquakes induced by a triple round-the-world echo. For another, the coincidence of the three aftershocks with the activity peaks of weaker aftershocks

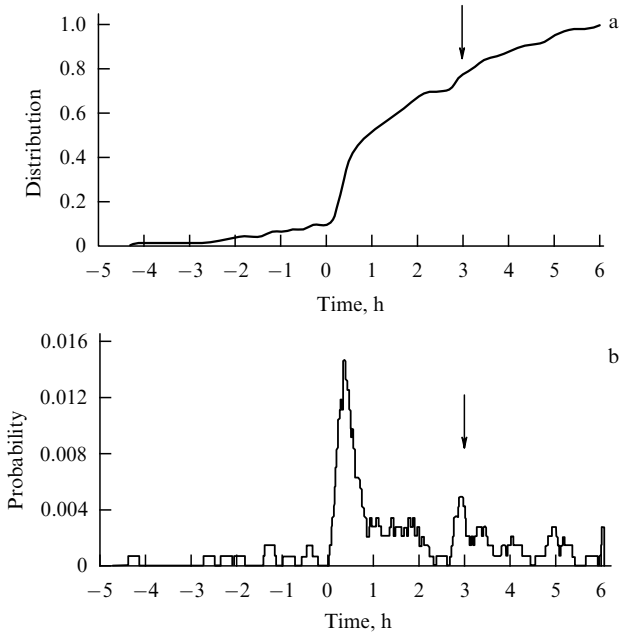

Figure 14. Dynamics of foreshocks and aftershocks with magnitudes $6 \leqslant M < 7.5$ in epicentral zones of 167 earthquakes with magnitude $M \geqslant 7.5$. The arrows point at the anticipated delay time of the round-the-world echo of a surface wave. (a) The distribution function of earthquakes over time with respect to their reference. (b) The probability density for earthquake appearance as a function of time.

provides arguments to hypothesize, with due caution, that we are dealing with the modulation of seismicity by free oscillations of Earth at the frequency of ~ 0.1 mHz.

4.2 Statistical analysis

The hypothesis claiming that the strongest aftershock of the Sumatra–Andaman earthquake was induced by a round-the-world seismic echo is backed by theoretical considerations and the analysis of aftershocks of the Tohoku earthquake. This alone would perhaps be insufficient if not for the presence of an additional, more conclusive argument, provided by the results of a statistical analysis of aftershock series for strong earthquakes [35, 36].

Figure 14 illustrates the dynamics of aftershocks in the interval of 6 h after 167 earthquakes with magnitudes $M \geqslant 7.5$ based on the data of the USGS catalogue from 1973 to 2010. The occurrence times of earthquakes with magnitudes $M \geqslant 7.5$ were used as references to synchronize the aftershocks with magnitudes $6 \leqslant M < 7.5$ in epicentral zones 2° in radius. Figure 14a displays a smoothed distribution of earthquakes over time relative to their references. Smoothing represents a running mean within an interval of 15 min applied with a step of 1 min. By differentiating the smoothed distribution, the probability density of an earthquake appearance was obtained, as demonstrated in Fig. 14b. We see that the maximum in aftershock activity is observed within the first hour after a strong earthquake. It is followed by a relatively quiescent interval, and then the activity begins to grow, ending in a new maximum of aftershock activity in approximately three hours. This observation lends additional support to our idea that surface elastic waves excited by the mainshock circumscribe Earth and, upon returning to the vicinity of the epicenter, may cause a strong aftershock there.

To conclude this section, we return to Fig. 7b, which plots a powerful energy release by aftershocks. The energy reaches

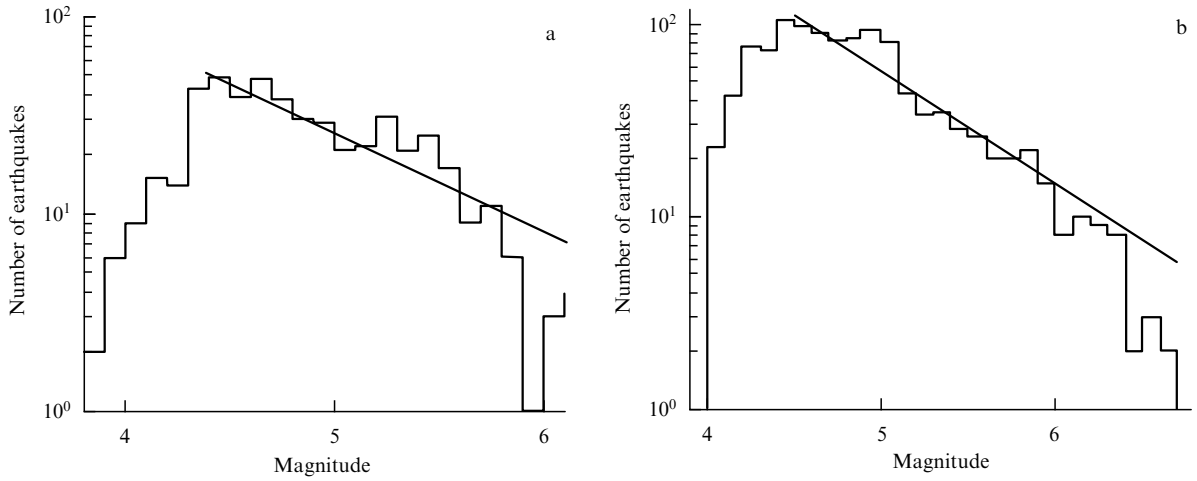

Figure 15. Distribution of aftershocks of the Sumatra–Andaman earthquake (a) and the Tohoku earthquake (b) over magnitudes in the interval of 50 h past the mainshocks in epicentral zones 10° in radius. The straight lines approximate the representative parts of respective catalogues.

11 PJ as a maximum approximately three hours after the reference. This agrees with the idea on the effect of the round-the-world echo of the mainshock on the 'cooling' earthquake source zone. Something similar is also seen in Fig. 8. A certain symmetry in energy release by foreshocks and aftershocks with respect to the instant of time of the mainshock is noteworthy. Here, we mean that the peaks in energy release are observed approximately three hours prior to and after the instant of the mainshock. This is of immense interest. We know that the round-the-world echo of a mainshock can stimulate the occurrence of a strong aftershock three hours after the mainshock. An assumption invites itself that the echo signals from foreshocks, which form the peak in energy release at the instant of time falling on -3 h, trigger the mainshocks, of the same manner as echo signals from mainshocks serve as triggers for aftershocks forming energy release peak at the instant $+3$ h. It cannot be ruled out that at least a part of strong earthquakes is excited in this way.

5. Modulation of seismicity with Earth's spheroidal oscillations

5.1 Analysis of the strongest earthquakes

It should be kept in mind that the concept of a round-the-world echo, introduced in Section 2, served as the basis for the search for the cumulative effect in antiepicenters of strong earthquakes. The result of this endeavor is shown in Fig. 9. It is seen that the effect is detectable only for the set of rather weak earthquakes. It has become clear in the analysis that the antiepicenters of earthquakes are located, as a rule, in aseismic areas. This explains why the effect is weak. However, more importantly, the aseismicity of antiepicenters hints at the idea of looking for a cumulative effect in the vicinities of the epicenters of strong earthquakes.

We returned to Fig. 9 not only to recall the logic of the development of research on the cumulative action of converging seismic waves on Earth's crust, but also because in Fig. 9 we see surprising oscillations with a quasiperiod of approximately 50 min in addition to the maximum in the activity of weak shocks discovered 90 min after the reference. These oscillations, discovered by chance [35], have no direct relation to the nonlinear antipodal effect. However, we draw attention to the closeness of the 50-min period to the fundamental period of spheroidal oscillations ${}_0S_2$, discovered by Benioff in the middle of the 1950s after a strong Kamchatka earthquake. The exact value of the period of ${}_0S_2$ oscillations comprises 54 min (see, for example, Refs [14, 45, 50]). This provides a rationale for a conjecture on the seismicity modulation with Earth's spheroidal oscillations. According to arguments discussed in detail in Sections 3 and 4, in order to test this hypothesis, it is reasonable to invoke observations of aftershocks in the vicinities of epicenters of strong earthquakes, rather than in the vicinities of antiepicenters.

Consider the aftershocks of the Sumatra–Andaman earthquake [36]. In the Introduction, while discussing the role of triggers, we mentioned that the probability of critical transition in a dynamical system sharply increases upon switching on an external periodic action, even if the exerted force is relatively weak [40]. As applied to the Sumatra–Andaman earthquake, we identify the periodic trigger with the spheroidal oscillations which were excited by the mainshock, and try to find the resonance frequency in the spectrum of aftershock series. The resonance frequency of the fundamental ${}_0S_2$ mode equals 0.309 mHz, which corresponds to the period of 54 min.

We begin by selecting from the USGS catalogue all aftershocks in the 50-h interval following the Sumatra–Andaman earthquake in the epicentral zone 10° in radius, and single out the so-called representative part. (See Ref. [56] on the importance of using a representative sampling in exploring earthquakes.) Figure 15a plots the distribution of aftershocks over magnitudes, and the straight line $\lg N = 4.0 - 0.5M$ approximates the representative part of the catalogue, which corresponds to magnitudes $M > 4.4$ and comprises 357 events. Here, N is the number of aftershocks with a given value of M. The correlation coefficient between N and M reaches 0.85 for the representative part. In what follows, we will also need a similar distribution for the Tohoku earthquake (Fig. 15b). The straight line $\lg N = 4.67 - 0.58M$ approximates the representative part of the catalogue, which corresponds to magnitudes $M > 4.4$ and contains 720 events. The correlation coefficient in this case reaches 0.916.

We will set up a correspondence between zero and every second of the interval selected for the analysis if there were no

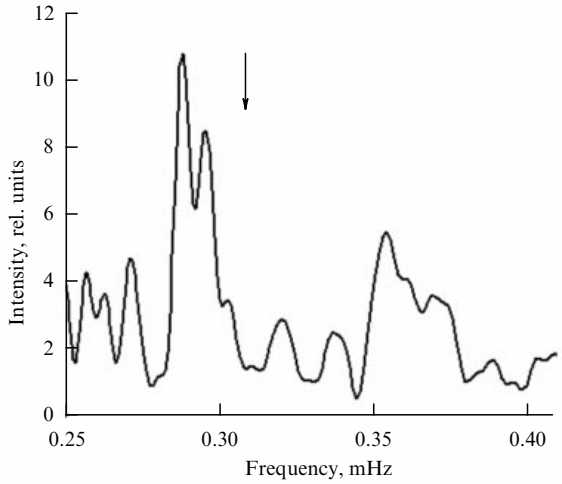

Figure 16. Spectrum of activity of aftershocks with magnitude $M > 4.4$ over the interval of 50 h after the Sumatra–Andaman earthquake in the epicentral zone 10° in radius. The arrow marks the frequency of fundamental mode ${}_0S_2$ of Earth's eigenoscillations.

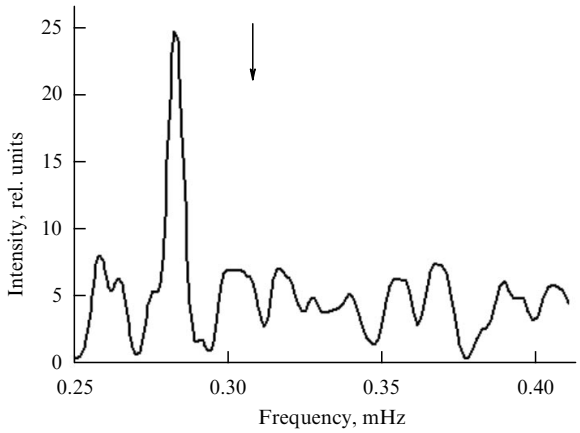

Figure 17. Spectrum of activity of aftershocks with magnitude $M > 4.4$ over the interval of 50 h after the earthquake in the Tohoku area in the epicentral zone 10° in radius. The arrow marks the frequency of fundamental mode ${}_0S_2$ of Earth's eigenoscillations.

earthquakes at a given second in the epicentral zone according to catalogue, or between the integer positive number v_j if there were v_j earthquakes from the representative part of the sample. In order to carry out a spectral analysis, we present the dynamics of aftershocks as a following series:

$$n(t) = \sum_{j=1}^{N} v_j \, \delta(t - t_j) \, . \tag{7}$$

Here, t_j is the beginning of one-second interval associated with v_j, and N is the total number of such intervals. We represent the function $n(t)$ in the form of a Fourier integral:

$$n(t) = \int_{-\infty}^{\infty} n_\omega \exp(-\mathrm{i}\omega t) \, \frac{\mathrm{d}\omega}{2\pi} \, . \tag{8}$$

The spectral component n_ω in expression (8) is defined by the formula

$$n_\omega = \int_{-\infty}^{\infty} n(t) \exp(\mathrm{i}\omega t) \, \mathrm{d}t \, . \tag{9}$$

Substituting expansion (7) into Eqn (9) yields

$$n_\omega = \sum_{j=1}^{N} v_j \exp(\mathrm{i}\omega t_j) \, . \tag{10}$$

Figure 16 plots the frequency dependence of the intensity $|n_\omega|^2$ of Fourier components. The arrow marks the frequency of spheroidal oscillations ${}_0S_2$. We detect a substantial increase in intensity in the frequency band 0.28–0.3 mHz, with the center of the band deviating from the frequency of spheroidal oscillations within only several percent. This indicates, in all probability, that Earth's spheroidal oscillations excited by the mainshock modulate the activity of aftershocks. The deviation just mentioned can be related to the error in estimating the intensity of the spectral components computed over a rather short realization of an earthquake series.

We strengthen our assumption through the analysis of aftershock activity after the earthquake in the Tohoku area. The frequency dependence of the intensity $|n_\omega|^2$ of Fourier components is plotted in Fig. 17, where the arrow, as earlier, indicates the frequency of spheroidal oscillations ${}_0S_2$. A prominent maximum at a frequency of 0.285 mHz deviates by only a few percent from the frequency of spheroidal oscillations, but this deviation may also be connected to the inaccuracy of estimating the spectral component intensity. Thus, we obtained one more indirect confirmation of the hypothesis of seismic activity modulation with Earth's spheroidal oscillations.

5.2 Statistical analysis

We augment the analysis of concrete events by the statistical analysis of a large number of earthquakes which took place over a long period. We use the data on global seismicity from 1973 to 2010 contained in the USGS catalogue. These data were split into four groups based on the minimum earthquake magnitude, and into four groups based on the maximum magnitude. For each group, the spectrum was computed as described in Section 5.1.

The calculated result is given in Fig. 18, where the values of minimum (Fig. 18a–d) and maximum (Fig. 18e–h) magnitudes and the series sizes are mentioned. The thin vertical lines indicate the frequency of the fundamental mode of Earth's spheroidal oscillations. The spectral pattern looks ambiguously only for $M < 4$ (Fig. 18g). In all other spectra, there is a clearly dominant peak at a frequency of 0.309 mHz ($M < 2$) or 0.307 mHz ($M > 4$), or peaks occur at both frequencies ($M > 1, 2, 3$ and $M < 6, 8$). Apparently, Fig. 18 provides a persuading confirmation of the modulation of global seismicity with spheroidal oscillations of Earth.

The peak at the frequency of 0.309 mHz coincides with the frequency of the fundamental mode of Earth's oscillations. The second peak is shifted by 0.002 mHz down, i.e., by less than 1%. Possibly, this small deviation is immaterial, being the consequence of the limited size of the series. However, it is worthwhile to pay attention to an interesting aspect of Fig. 18. We see that, in moving from Fig. 18d ($M > 1$) to Fig. 18a ($M > 4$), the left part of the split spectrum monotonically increases. This feature resembles the spectral energy flux in forced oscillations of a nonlinear system. It is well known that the superposition principle is inapplicable in the nonlinear theory of oscillations. The spectrum of oscillations may deviate from that of external action even if the latter is

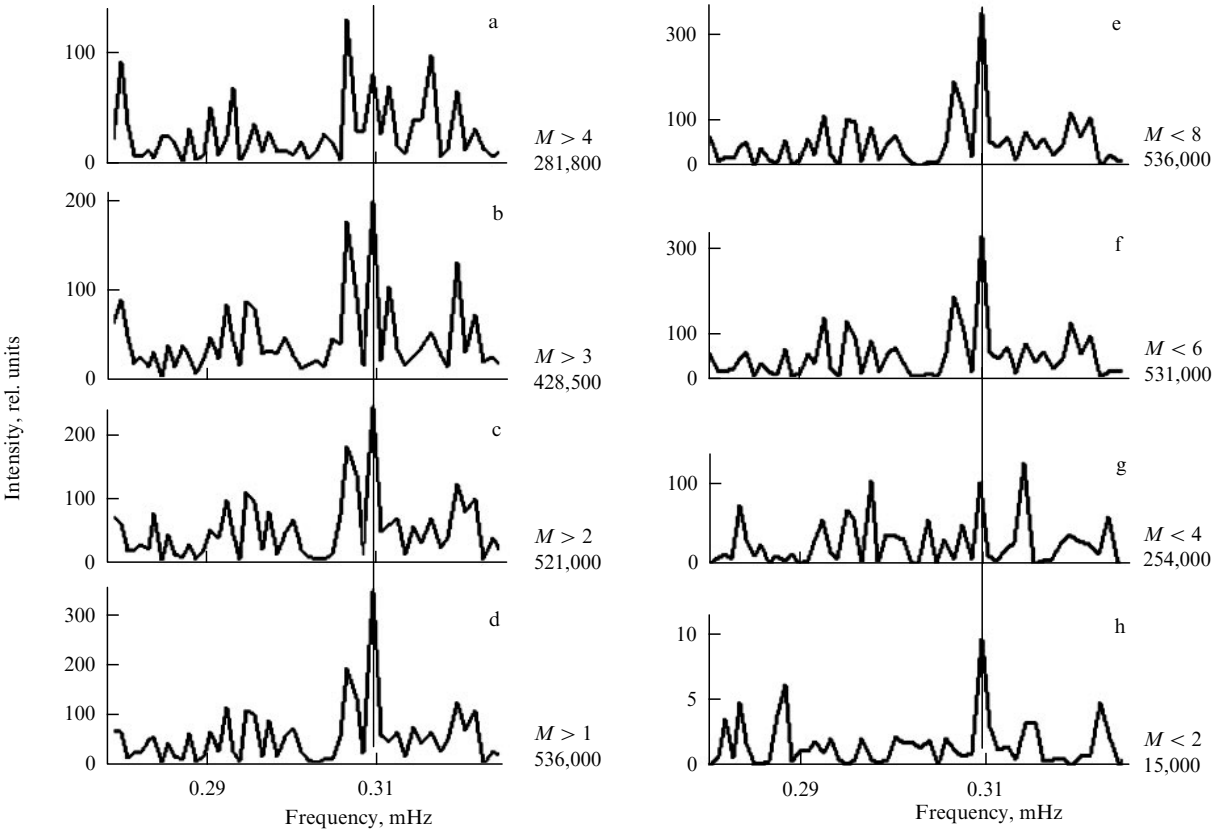

Figure 18. Spectra of global seismicity from 1973 to 2010.

strictly sinusoidal. This invites the question of whether the small shift of the maximum in the spectrum of aftershocks of the strongest Sumatra–Andaman earthquake with respect to the frequency of the exciting force (see Fig. 16) is the result of nonlinear transformation of the spectrum of Earth's spheroidal oscillations. We cannot propose an answer to this question yet.

To conclude this section, we note that to find the spectral peak with a period of 54 min more than a half million events have been processed, covering several decades. This has utilized practically all information available now for studies with the method based on the analysis of earthquake catalogues. Further research, the need for which is dictated by the nontrivial character and novelty of the problem, should resort to more elaborate methods of seismology.

6. Discussions

After occurring the mainshock, relaxation processes come about in the epicentral zone. One can metaphorically say that the epicentral zone is cooling down. This process in no way resembles the gradual cooling of a heated homogeneous body. In contrast, in the epicentral zone, which represents a strongly nonlinear, structured system, complex processes continue to unfold, with long incessant activity of aftershocks being one of the consequences.

In all probability, all aftershocks appear spontaneously, excluding the one triggered by the round-the-world echo of the mainshock. Its anomalously high amplitude has been considered in Ref. [36] as a distinguishing feature allowing one to single out this aftershock among others. We agree to refer to such an aftershock as a strong aftershock (SAS). But, judging by the available knowledge, an anomalously large magnitude is a sufficient but not necessary feature, so that the abbreviation SAS can also stand for a special or strange aftershock.

Is it possible by observing SASs to retrieve useful information on physical processes in the cooling earthquake epicentral zone? It would be incorrect to abandon such a possibility, because SASs fall into a class of extreme events and present a nontrivial reaction of a dynamical system to an external pulse action. We list parameters of an SAS that might be of interest for diagnostics of this kind. First of all, they include geometric parameters: the distance between the epicenters, the mutual orientation of epicenters, and the difference in depths between hypocenters of the mainshock and the SASs. They are followed by two energy parameters: the ratio of SAS magnitude to that of the mainshock and to the mean magnitude of the sequence of aftershocks, in the temporal vicinity of the SASs. Finally, it is necessary to pay attention to the difference δt between the operating time of the trigger, which is the front of the round-the-world echo, and the time the front arrived at the SAS hypocenter.

The geometrical and energy parameters of SASs can be readily measured by standard seismologic methods, but measuring δt requires a special approach. A rough estimate of the quantity δt is given by the difference between the time an SAS was excited and the computed time of the round-the-world seismic echo arrival. For example, for the Sumatra–Andaman earthquake, the SAS occurred 3 h 20 min after the mainshock. If we take for the mean propagation speed 3.7 km s^{-1} along its path, we estimate $\delta t = 20$ min. However, this estimate may only serve for orientation, for there is scatter in the surface wave propagation speeds.

Without going into detail, we would only like to stress the promising character of nonlinear sounding of earthquake source zones based on the data on SASs. The quantity δt is of special interest, because it can be used as an important kinematic parameter reflecting the delay in nonlinear reaction in the earthquake source zone to the controlled external action. It seems useful to study the dependence of δt on the earthquake magnitude, the depth of the hypocenter, and the local detail of the lithosphere.

In its time, a consensus formed in geophysics that in practice there are no similar geomagnetic storms. Each has its specific features which are set by a unique combination of a large number of local and global parameters of the near-terrestrial medium. Seemingly, the same concerns strong earthquakes, because the inception and activation of the seismic center depend on a rich variety of physical conditions in seismogenic structures of Earth's crust [57]. In this respect, it seems important to study through observations the probability of SAS excitation as a function of tectonic position and geological structure of the epicentral zone.

We now briefly discuss the cumulative effect from the standpoint of magnetology. Earlier, in the framework of seismoelectrodynamics [58], the excitation of magnetic oscillations by seismic waves leaving the earthquake source zone was discussed. The experimental search for and theoretical modeling of strong magnetic field pulses excited upon the focusing of converging waves are doubtless of interest. One more important area pertains to studies of antipodal magnetic anomalies formed on the Moon and Mercury in the collisional magnetization of rock structures in the remote past.

Finally, we touch on the modulation of global seismicity with Earth's free oscillations. The spectra in Fig. 18 look like a sufficiently reliable argument confirming the reality of the modulation effect. Could it be possible to use this phenomenon in astroseismology, and, in particular, in pulsar seismology? Why not try singling out resonance peaks in the sequence of pulsarquakes and in that way estimate the periods of pulsar elastic oscillations? However, observational series of sufficient length are still unavailable.

7. Conclusions

It is well known that there are 'eternal questions' in science which incessantly pique one's interest and simulate searching for a certain answer. Such questions exist in geophysics, too. They include, for example, the question about the equation of state in Earth's core and a broad set of unsolved questions of the physics of earthquakes. The most difficult one is considered to be on the mechanism of earthquakes with a deep focus. Such earthquakes sometimes take place not in the lithosphere, as they usually do, but in plastic layers of the mantle. The interest in deep-focus earthquakes gained a new impetus recently, through the earthquake on 24 May 2013, with magnitude $M = 8.2$, epicenter in the Sea of Okhotsk, and the hypocenter at a depth of 600 km.

Many questions related to lithospheric earthquakes with hypocenters at depths of less than 70 km are widely discussed by the geophysical community. Thus far, no one has succeeded in proposing a self-consistent theory of earthquakes resting on first principles. The vast observational material is commonly analyzed in frameworks of phenomenological models, imitating some sides of the process of stress accumulation and mainline rupture of rock continuity. Staying with this tendency, we used in this paper catastrophe theory along with ideas and concepts of the theory of fluctuations and critical phenomena to analyze foreshocks and aftershocks of strong earthquakes.

Our attention was concentrated on simple and robust characteristics of critical transitions. We appealed to the elevated reactivity of dynamical systems in a near-threshold domain, oscillation frequency reduction for some modes, the increase in correlation lengths, and other anomalous phenomena that are related to critical opalescence. In the absence of a sufficiently complete theory of earthquakes, these ideas can naturally be used as a basis for analyzing observations. As a result, we managed to discover a set of nontrivial characteristics of the earthquake source zone prior to and after the mainline rupture. In the course of the analysis of foreshocks and aftershocks, we introduced the concept of the round-the-world seismic echo, of the cumulative effect of converging surface waves in the epicentral vicinity, and of modulation of global seismicity with free oscillations of the Earth. Further research in these areas seems both interesting and promising.

Acknowledgments

The problem of foreshocks has been repeatedly discussed by the author with L E Sobisevich and A L Sobisevich, and the problem of aftershocks with A D Zavyalov. O D Zotov and I P Lavrov significantly helped both in research and in preparing the article for publication. The author expresses his deep gratitude to all of them. The work was carried out in the framework of Program No. 18 of the Presidium of the RAS on Fundamental Research and with support from RFBR (projects Nos 13-05-00066, and 15-05-00491).

References

1. Bolt B A *Earthquakes* (San Francisco: W.H. Freeman, 1978); Translated into Russian: *Zemletryaseniya* (Moscow: Mir, 1981)
2. Richter C F *Elementary Seismology* (San Francisco: W.H. Freeman, 1958); Translated into Russian: *Elementarnaya Seismologiya* (Moscow: IL, 1963)
3. Kasahara K *Earthquake Mechanics* (Cambridge: Cambridge Univ. Press, 1981); Translated into Russian: *Mekhanika Zemletryasenii* (Moscow: Mir, 1986)
4. Båth M *Tectonophysics* **2** 483 (1965)
5. Gutenberg B, Richter C F *Bull. Seismol. Soc. Am.* **34** 185 (1944)
6. Mogi K *Earthquake Prediction* (Tokyo: Academic Press, 1985); Translated into Russian: *Predskazanie Zemletryasenii* (Moscow: Mir, 1988)
7. Sobolev G A *Osnovy Prognoza Zemletryasenii* (Fundamentals of Earthquake Prediction) (Moscow: Nauka, 1993)
8. Zav'yalov A D *Priroda* (5) 29 (2005)
9. Dunbar P et al. *Geomatics Natural Hazards Risk* **2** 305 (2011)
10. Krylov A N *Usp. Fiz. Nauk* **1** 101 (1918)
11. Leet L D *Am. Scientist* **34** 198 (1946); *Usp. Fiz. Nauk* **31** 264 (1947)
12. Sytinskii A D *Sov. Phys. Usp.* **16** 740 (1973); *Usp. Fiz. Nauk* **111** 367 (1973)
13. Buchachenko A L et al. *Phys. Usp.* **39** 959 (1996); *Usp. Fiz. Nauk* **166** 1023 (1996)
14. Kuznetsov V V *Phys. Usp.* **40** 951 (1997); *Usp. Fiz. Nauk* **167** 1001 (1997)
15. Fridman A M, Polyachenko E V, Nasyrkanov N R *Phys. Usp.* **53** 291 (2010); *Usp. Fiz. Nauk* **180** 303 (2010)
16. Buchachenko A L *Phys. Usp.* **57** 92 (2014); *Usp. Fiz. Nauk* **184** 101 (2014)
17. Kalashnikov A G *Tr. Geofiz. Inst. Akad. Nauk SSSR* **25** 180 (1954)
18. Fraser-Smith A C et al. *Geophys. Res. Lett.* **17** 1465 (1990)
19. Sobolev G A, Ponomarev A V *Fizika Zemletryasenii i Predvestniki* (Physics of Earthquakes and Precursors) (Moscow: Nauka, 2003)

20. Hattori K *Terr. Atmos. Oceanic Sci.* **15** 329 (2004)
21. Pulinets S *Terr. Atmos. Oceanic Sci.* **15** 413 (2004)
22. Dovbnya B V *J. Atmos. Solar-Terr. Phys.* **69** 1765 (2007)
23. Hayakawa M *Sensors* **7** 1141 (2007)
24. Sobisevich L E, Sobisevich A L *Vestn. Otd. Nauk o Zemle Ross. Akad. Nauk* **2** 202 (2010)
25. Sobisevich L E, Kanonidi K Kh, Sobisevich A L *Dokl. Earth Sci.* **435** 1627 (2010); *Dokl. Ross. Akad. Nauk* **435** 548 (2010)
26. Guglielmi A V, Zotov O D *Izv. Phys. Solid Earth* **48** 171 (2012); *Fiz. Zemli* (2) 84 (2012)
27. Zotov O D, Guglielmi A V, Sobisevich A L *Izv. Phys. Solid Earth* **49** 882 (2013); *Fiz. Zemli* (6) 139 (2013)
28. Thom R *SIAM Rev.* **19** 189 (1977)
29. Gilmore R *Catastrophe Theory for Scientists and Engineers* (New York: Wiley, 1981); Translated into Russian: *Prikladnaya Teoriya Katastrof* (Moscow: Mir, 1984)
30. Arnold V I *Catastrophe Theory* (Berlin: Springer-Verlag, 1992); Translated from Russian: *Teoriya Katastrof* (Moscow: Nauka, 1990)
31. Zubkov L A, Romanov V P *Sov. Phys. Usp.* **31** 328 (1988); *Usp. Fiz. Nauk* **154** 615 (1988)
32. Guglielmi A V *Sov. Phys. Usp.* **32** 678 (1989); *Usp. Fiz. Nauk* **158** 605 (1989)
33. Guglielmi A V, Pokhotelov O A *Geoelectromagnetic Waves* (Bristol: Institute of Physics Publ., 1996)
34. Guglielmi A, Zotov O, arXiv:1207.0365
35. Guglielmi A V, Zotov O D *Izv. Phys. Solid Earth* **49** 1 (2013); *Fiz. Zemli* (1) 3 (2013)
36. Guglielmi A V, Zotov O D, Zavyalov A D *Izv. Phys. Solid Earth* **50** 64 (2014); *Fiz. Zemli* (1) 66 (2014)
37. Guglielmi A V et al. *Izv. Phys. Solid Earth* **50** 501 (2014); *Fiz. Zemli* (4) 43 (2014)
38. Horsthemke W, Lefever R *Noise-Induced Transitions* (Berlin: Springer-Verlag, 1984)
39. Kramers H A *Physica* **7** 284 (1940)
40. Smelyanskiy V N, Dykman M I, Golding B *Phys. Rev. Lett.* **82** 3193 (1999)
41. Avsyuk Yu N *Prilivnye Sily i Prirodnye Protsessy* (Tidal Forces and Processes in the Nature) (Moscow: OIFZ RAN, 1996)
42. Adushkin V V, Turuntaev S B *Tekhnogennye Protsessy v Zemnoi Kore* (*Opasnosti i Katastrofy*) [Technogenic Processes in the Earth's Crust (Dangers and Catastrophes)] (Moscow: INEK, Institut Dinamiki Geosfer RAN, 2005)
43. Sobolev G A *Natural Hazards Earth Syst. Sci.* **11** 445 (2011)
44. Gurevich A V, Tsedilina E E *Long Distance Propagation of HF Radio Waves* (Berlin: Springer-Verlag, 1985); Translated from Russian: *Sverkhdal'nee Rasprostranenie Korotkikh Radiovoln* (Moscow: Nauka, 1979)
45. Zharkov V N *Fizika Zemnykh Nedr* (Physics of Earth's Interior) (Moscow: Nauka i Obrazovanie, 2012)
46. Gradshteyn I S, Ryzhik I M *Tables of Integrals, Series and Products* (New York: Academic Press, 1965); Translated from Russian: *Tablitsy Integralov, Summ, Ryadov i Proizvedenii* (Moscow: GIFML, 1962)
47. Babič V M, Buldyrev V S *Short-Wavelength Diffraction Theory*: *Asymptotic Methods* (Berlin: Springer-Verlag, 1991); Translated from Russian: *Asimptoticheskie Metody v Zadachakh Difraktsii Korotkikh Voln* (Moscow: Nauka, 1972)
48. Zel'dovich Ya B, Novikov I D *Stroenie i Evolyutsiya Vselennoi* (The Structure and Evolution of the Universe) (Moscow: Nauka, 1975) p. 711
49. Feynman R P *Science* **153** 699 (1966); "The development of the space-time view of quantum electrodynamics", Nobel Lecture, December 11, 1965. Preprint les Prix Nobel en 1965 (Stockholm: The Nobel Foundation, 1966); *Usp. Fiz. Nauk* **91** 29 (1967)
50. Aki K, Richards P G *Quantitative Seismology* (San Francisco: W.H. Freeman, 1980); Translated into Russian: *Kolichesvennaya Seismologiya* (Moscow: Mir, 1983)
51. Al'pert Ya L *Sov. Phys. Usp.* **3** 479 (1961); *Usp. Fiz. Nauk* **71** 369 (1960)
52. Samson J C, Yeung K L *Planet. Space Sci.* **34** 1133 (1986)
53. Schultz P H, Gault D E *Moon* **12** 159 (1975)
54. Blewett D T et al. *Icarus* **209** 239 (2010)
55. Lü J et al. *Planet. Space Sci.* **59** 1981 (2011)
56. Smirnov V B *Vulkanologiya Seismologiya* (4) 93 (1997)
57. Rogozhin E A *Ross. Zh. Nauk Zemle* **2** (1) 37 (2000)
58. Guglielmi A V *Phys. Usp.* **50** 1197 (2007); *Usp. Fiz. Nauk* **177** 1257 (2007)